



# Polyaniline-coated reduced graphene oxide as an efficient adsorbent for the removal of malachite green from water samples

Armaghan Ghahramani<sup>1</sup> · Mohammad Gheibi<sup>2</sup> · Mohammad Eftekhari<sup>3</sup>

Received: 2 August 2018 / Revised: 28 November 2018 / Accepted: 7 December 2018 /

Published online: 11 December 2018

© Springer-Verlag GmbH Germany, part of Springer Nature 2018

## Abstract

An efficient and novel reduced graphene oxide–polyaniline (rGO–PANI) nanocomposite was used for highly rapid removal of malachite green (MG) from water samples. Graphene oxide was synthesized from graphite by Hummers' method, and after reduction to reduced graphene oxide by sodium borohydride ( $\text{NaBH}_4$ ), its surface was modified by polyaniline to synthesize rGO–PANI nanocomposite. Fourier transform infrared spectrophotometry (FT-IR), electron-dispersive spectroscopy (EDS) and scanning electron microscopy (SEM) were used to characterize the synthesized rGO–PANI nanocomposite. The important parameters affecting the removal efficiency such as pH, contact time and initial MG concentration were studied and optimized. Also, kinetic models including the pseudo-first- and second-order equations were investigated and kinetic parameters of the studied dye were calculated and discussed. It was shown that the adsorption of MG by rGO–PANI nanocomposite could be described by the pseudo-first-order kinetic equation. Also, the experimental isotherms data were analyzed using the Langmuir and Freundlich equations and based on the results, the adsorption of MG by rGO–PANI nanocomposite was followed by both Langmuir and Freundlich equations. The maximum adsorption capacities for MG were calculated and equal to  $666.7 \text{ mg g}^{-1}$  which shows that rGO–PANI nanocomposite is a very efficient adsorbent for the removal of MG from water samples.

**Keywords** Reduced graphene oxide–polyaniline nanocomposite · Malachite green · Removal · Kinetic models

---

✉ Mohammad Eftekhari  
meftekhari85@yahoo.com

<sup>1</sup> Department of Civil Engineering, Ferdowsi University of Mashhad, Mashhad, Iran

<sup>2</sup> Department of Civil and Environmental Engineering, Ferdowsi University of Mashhad, Mashhad, Iran

<sup>3</sup> Department of Chemistry, Faculty of Sciences, University of Neyshabur, Neyshabur, Iran

## Introduction

Environmental contaminants by dyes are of the major concern for living organism [1]. Introduction of colored dyes into the water samples causes prevention light penetration for aquatic plant, and therefore, by disruption of photosynthesis process, the concentration of dissolved oxygen which is necessary for living organism reduces dramatically [2]. Also most of dyes are toxic, causing allergies and skin irritation and in the case of azo dyes, their degradation by microorganism produces toxic, carcinogenic and mutagenic compounds [3]. Therefore, by considering the health risks and hazards of these chemicals, it is inevitable to remove dyes from water and wastewater samples. Malachite green (MG) is a cationic dye with widespread application in textile and also, although it is illegal, as an inexpensive antibacterial to treat *Saprolegnia* in fish and fungicide in aquaculture industry. However, it can cause skin sensitization or even skin cancer in the long term [4]. Among different methods developed for the removal of dyes from water samples, adsorption is one of the most common techniques due to its simplicity, variety of adsorbents, high efficiency and low costs.

Different adsorbents such as modified graphene oxide [5], magnetic reduced graphene oxide [6], activated carbon [7, 8], industrial wastes [9–11], functionalized carbon nanotubes [12], natural zeolite [13, 14] and green adsorbents [15–17] were used for the removal of MG. Graphene oxide (GO), which is produced by oxidation of graphite followed by exfoliation of graphite oxide, has many applications in different research fields due to its high surface area, availability, economical price, electrical conductivity and presence of functional groups to modify its surface [18–20]. Also, it was used as a precursor for production of graphene (G), a plane of  $sp^2$  carbon material [21]. In this regard, chemical reduction of GO is a commonly used method for the production of graphene or reduced graphene oxide (rGO) [22].

Conductive polymers such as polyaniline (PANI), polypyrrole (PPy) and polythiophene (PTh) have received great attention in different research fields in the last decade [23–27]. Their wide applications in modern advanced electronic device such as organic light emission diode, photovoltaics and electrochromic devices, sensors and solar cells cause improvement in their performance. Due to the simple synthesis route, availability, low cost, conductivity, doping/dedoping chemistry and stability, PANI has gained wide applications [28–30]. Its monomer unit is shown in Fig. 1 and consists of reduced ( $y$ ) and oxidized ( $1-y$ ) parts, where  $0 \leq y \leq 1$ . If  $y=0.5$ , polyaniline exists in emeraldine form;  $y=0$  is pernigraniline and  $y=1$  is the leucoemeraldine form [31–36].

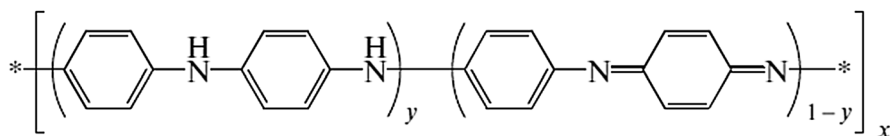


Fig. 1 Chemical Structures of polyaniline

In this research, Hummers' method was employed for synthesis of GO and it was used as a precursor for production of rGO using sodium borohydride ( $\text{NaBH}_4$ ) as a reducing agent. Polyaniline was then coated on the surface of rGO to synthesize rGO–PANI nanocomposite. After characterization of the synthesized adsorbent by FT-IR spectrophotometry, electron-dispersive X-ray spectroscopy (EDS) and scanning electron microscopy (SEM), it was used for the removal of MG from water samples. The main factors influencing the removal percentage such as pH and contact time were investigated and optimized. Finally, two kinetic models including pseudo-first- and second-order equations and also adsorption isotherms were studied and interpreted. The obtained results show that rGO–PANI nanocomposite is a very efficient adsorbent for the removal of MG from water samples and also, there is not any report for using rGO–PANI nanocomposite as an adsorbent for the removal of MG. Therefore, its high efficiency besides other advantages such as short removal time and cost-effectiveness makes it a unique adsorbent for the removal of MG from water samples.

## Materials and methods

### Material

Deionized water was used throughout the analysis. Malachite green chloride (Sigma Aldrich Company, USA) was used for the preparation of  $1000 \text{ mg L}^{-1}$  MG stock solution (0.1108 g of malachite green chloride was diluted with 100 mL of deionized water). The oxidation of graphite powder (Merck, Germany) to GO was performed by chemicals including  $\text{KMnO}_4$  (Merck, Germany),  $\text{H}_2\text{O}_2$  (Merck, Germany),  $\text{H}_2\text{SO}_4$  (98%, Merck, Germany) and  $\text{NaNO}_3$  (Fluka). A reducing agent  $\text{NaBH}_4$  was purchased from Sigma Aldrich Company (USA), and chemicals including ammonium persulfate ( $(\text{NH}_4)_2\text{S}_2\text{O}_8$ , Merck, Germany) and aniline (Merck, Germany) were used for synthesis of rGO–PANI nanocomposite.

### Instruments

The recording of UV–Vis spectrum was carried out within the range of 200–900 nm. An Agilent photodiode-array model 8453 was employed; this device is equipped with a 1-cm path length quartz cell. The measurements of pH were performed by Metrohm 827 pH lab (Switzerland), and the separation of adsorbent from sample solution was performed by a Centurion Centrifuge (Andreas Hettich D72, Germany). The morphology of rGO–PANI nanocomposite (SEM images) was determined by Philips XL30 ESEM FEG instrument (Philips Company, Netherlands). Also, Vector 22 spectrometer was used for recording FT-IR spectrum and EDS analysis was done by Oxford 7353 EDX microanalyzer.

## Synthesis of Graphene Oxide nanosheets

To synthesize GO from graphite powder, the Hummers' method was used according to our previous research paper [20]. To the 1 g of graphite powder, an aliquot of 23 mL  $\text{H}_2\text{SO}_4$  was added and stirred for 30 min at 5 °C. Then, 0.5 g  $\text{NaNO}_3$  was added to the mixture and stirred at 15–20 °C for 30 min. After addition of 3 g  $\text{KMnO}_4$  to the mixture during 1 h, the resulting mixture was stirred at 15–20 °C for 90 min and heated along with stirring at 35 °C for 120 min. Subsequently, 100 mL of deionized water was added to the mixture followed by addition of 5 mL  $\text{H}_2\text{O}_2$  to it to obtain green mixture. Then, the resulting graphite oxide was washed with deionized water for several times to obtain pH 7–8 for supernatant and ultrasonicated for 60 min to synthesize GO nanosheets. Finally, after centrifugation of the synthesized GO at 3500 rpm, it was dried at 60 °C for 12 h.

## Synthesis of rGO nanosheets

rGO nanosheets were synthesized by Shin et al. [37]. A mixture of 2.5 g  $\text{L}^{-1}$  GO in deionized water was ultrasonicated for 45 min. Then, a solution of 0.15 mol  $\text{L}^{-1}$   $\text{NaBH}_4$  was added to the mixture followed by stirring at 80 °C for 120 min. The synthesized rGO nanosheets were washed by deionized water for several times and dried at 60 °C for 12 h.

## Synthesis of rGO–PANI nanocomposite

The mixture of 1 g  $\text{L}^{-1}$  rGO was prepared in deionized water and ultrasonicated for 45 min. Then, 200  $\mu\text{L}$  of aniline was added to the mixture and stirred for 30 min at 400 rpm. By addition of 10 mL of 1%  $(\text{NH}_4)_2\text{S}_2\text{O}_8$  to the mixture, it was stirred for 120 min. Finally, the resulting rGO–PANI nanocomposite was centrifuged at 4000 rpm for 10 min and washed with deionized water for several times followed by drying at 60 °C for 12 h [38].

## Removal procedure

To the 50 mL of sample solution containing 2.5 mL of 1000 mg  $\text{L}^{-1}$  MG (50 mg  $\text{L}^{-1}$  MG) at the pH value of 6, an amount of 0.01 g rGO–PANI nanocomposite was added. The mixture was stirred at 400 rpm for 20 min at room temperature ( $25 \pm 2$  °C) by magnetic stirrer and centrifuged at 3500 rpm for 10 min. Finally, the absorbance of the remaining MG in the aqueous phase was determined by the standard calibration curve at 620 nm. The adsorption capacity for the rGO–PANI nanocomposite was determined as explained in Eq. 1:

$$q_e = \frac{(C_o - C_e)V}{W}, \quad (1)$$

where  $q_e$  is the adsorption capacity ( $\text{mg g}^{-1}$ ),  $C_0$  is the initial concentration of MG and  $C_e$  is the equilibrium concentrations of MG ( $\text{mg L}^{-1}$ );  $V$  is the volume of sample solution (L) and  $W$  is the amounts of rGO–PANI nanocomposite (g).

## Results and discussion

### Characterization of the synthesized rGO–PANI nanocomposite

The synthesized rGO–PANI nanocomposite was characterized by FT-IR spectroscopy, SEM images and EDS analysis. Figure 2 shows the FT-IR spectrum of the synthesized rGO and rGO–PANI nanocomposite. As it shows, the stretching vibration of benzenoid and quinonoid rings appeared at  $1490 \text{ cm}^{-1}$  and  $1571 \text{ cm}^{-1}$ , respectively; also, the peaks at  $1300 \text{ cm}^{-1}$  and  $1237 \text{ cm}^{-1}$  are related to the C=N and C–N stretching vibrations, respectively. Additionally, the peaks at  $1137 \text{ cm}^{-1}$  and  $3300 \text{ cm}^{-1}$  are related to the bending vibration of the C–H bands in the aromatic ring and N–H stretching mode, respectively [38–40]. Also, the result of EDS analysis on rGO–PANI nanocomposite is presented in Fig. 3. As it could be seen, the presence of N atom in the spectrum confirms that rGO–PANI nanocomposite has been synthesized successfully. Finally, the morphology of the synthesized rGO–PANI nanocomposite was determined by SEM images and is presented in Fig. 4. Based on the results, PANI has covered rGO nanosheets successfully. Therefore, all results show that rGO–PANI nanocomposite has been successfully synthesized.

### Effect of pH

The pH of sample solution causes change in the net charge of adsorbent which is related to its effect on the protonation/deprotonation of functional groups existing on the adsorbent. The effect of sample pH on the adsorption capacity of MG was investigated in

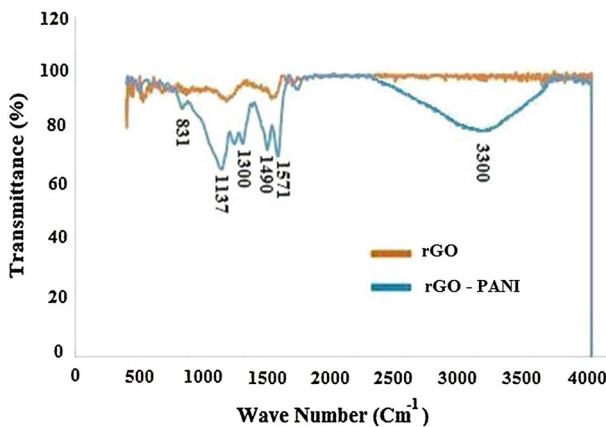


Fig. 2 FT-IR spectrum of the synthesized rGO–PANI nanocomposite

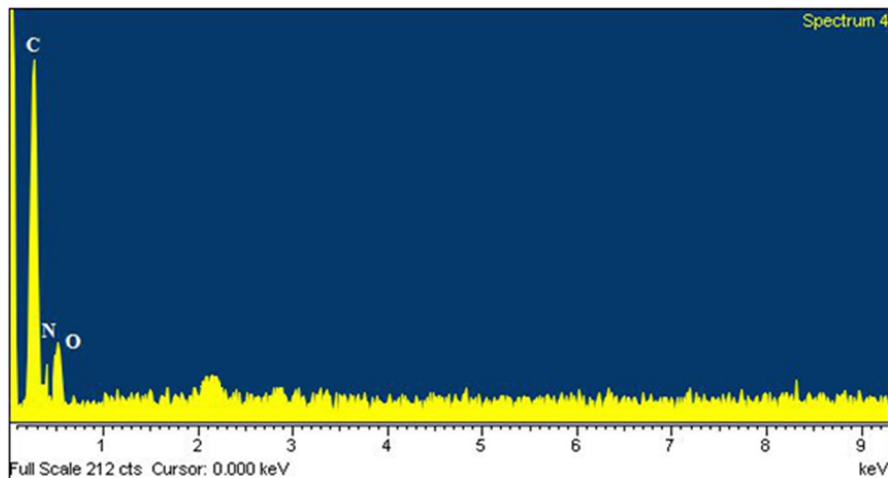
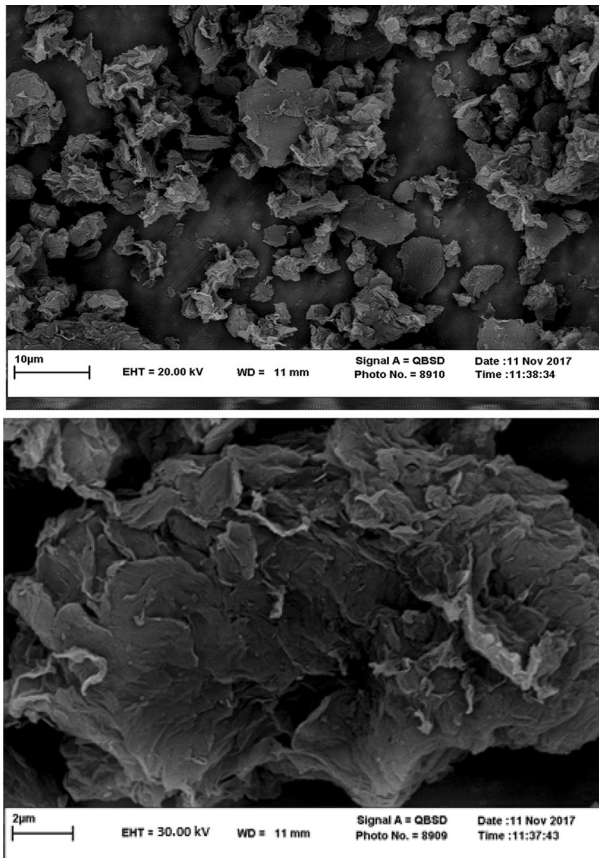


Fig. 3 EDS analysis on the synthesized rGO–PANI nanocomposite

the range of 3–9 at room temperature, and the obtained results are presented in Fig. 5. As the results show, the adsorption capacity of MG increases by increase of pH and it reaches its maximum value at  $\text{pH} > 5$ . At the pH values less than 3.5 ( $\text{pH}_{\text{PZC}}$ ), the nitrogen atoms of PANI molecules were protonated and the coulombic repulsion of rGO–PANI nanocomposite and MG molecules causes the decrease of adsorption capacity of MG. The results of zeta potential at pH values of 3, 4, 5, 6, 8 and 9 are +5.6, –6.2, –10.8, –19.5 and –23.2 mV, respectively; and these results obviously show that at low pH values (below than 4), the surface of rGO–PANI nanocomposite has positive charge. Therefore, for further experiments, pH 6 was selected as the optimum.

### Effect of contact time and initial concentration of MG

The effect of contact time on the adsorption capacity of MG was investigated in the time interval of 10–120 min for different concentrations of MG. The obtained results are presented in Fig. 6. Based on the results, the maximum adsorption capacity for MG was reached just at 20 min contact time and it remains constant afterward. Also, the results in Fig. 6 show that increase of MG concentration at constant temperature and stirring rate causes the increase of adsorption capacity of MG which could be related to the acceleration of diffusion process of MG from the solution onto the rGO–PANI surface. These results show that rGO–PANI is a high-speed adsorbent for the removal of MG from water samples.



**Fig. 4** SEM images of the synthesized rGO–PANI nanocomposite

### Adsorption isotherms

In this research, two common adsorption isotherms including Langmuir and Freundlich were investigated in detail to understand the adsorption behavior of MG onto the rGO–PANI nanocomposite.

### Langmuir and Freundlich

The Langmuir equation is valid for the monolayer sorption of MG onto the rGO–PANI nanocomposite. Equation 2 shows the linear form of the Langmuir equation. Therefore, by depiction of  $C_e/q_e$  versus  $C_e$ , the values of  $Q_{\max}$  (theoretical maximum adsorption capacity,  $\text{mg g}^{-1}$ ) and  $K_{\text{ads}}$  (Langmuir constant,  $\text{mg L}^{-1}$ ) could be calculated from the slope and intercept of the resulting plot, respectively (Table 1). According to the obtained  $Q_{\max}$  ( $666.7 \text{ mg g}^{-1}$ ), it could be expected that rGO–PANI nanocomposite is

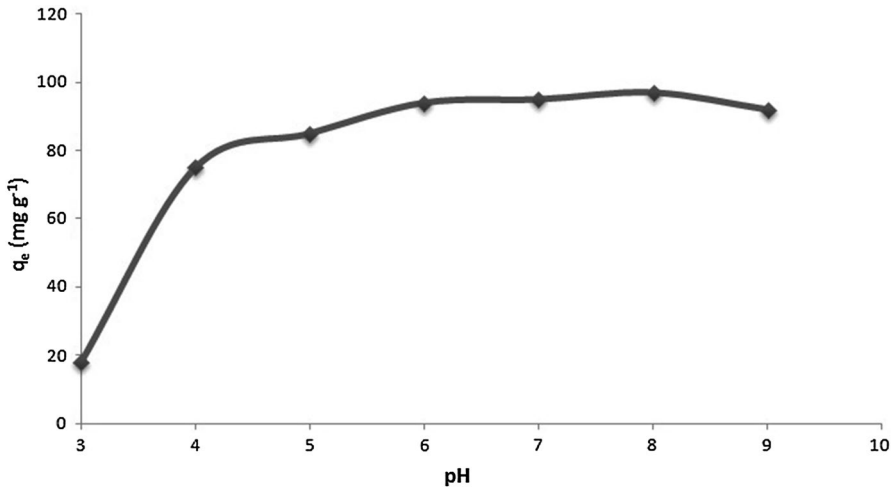


**Fig. 5** Effect of pH on the adsorption capacity of MG on the rGO-PANI nanocomposite. Conditions: 50 mg L<sup>-1</sup> MG, contact time: 20 min and room temperature (25 ± 2 °C)

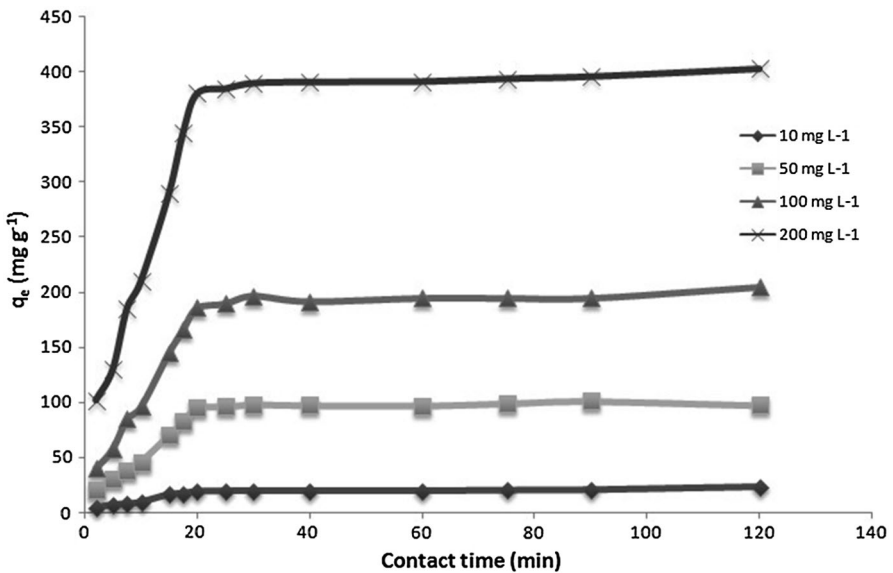


**Fig. 6** Effect of contact time and initial MG concentration on the adsorption capacity of MG onto the rGO-PANI. Conditions: pH: 6 and room temperature (25 ± 2 °C)

an efficient and powerful adsorbent for the removal of MG from water samples. Also, by using rGO alone as adsorbent, the obtained theoretical  $Q_{\max}$  was 353 mg g<sup>-1</sup>. The obtained results show that by modification of rGO with PANI molecules, the adsorption capacity of adsorbent improves impressively.

$$C_e/q_e = C_e/Q_{\max} + K_{\text{ads}}/Q_{\max} \quad (2)$$



**Table 1** Isotherm parameters for the adsorption of MG with rGO–PANI nanocomposite

Model	Parameter	Parameter value
Langmuir	$Q_m$ (mg g <sup>-1</sup> )	666.7
	$K_{ads}$	6.9
	$R^2$	0.98
Freundlich	$1/n$	0.92
	$K_f$	9.7
	$R^2$	0.97

The experimental maximum adsorption capacity for rGO–PANI nanocomposite which could be determined by depiction of  $q_e$  versus  $C_e$  is equal to 384.8 mg g<sup>-1</sup> MG [20] (Fig. 7).

The linear form of Freundlich equation which is valid for multilayer adsorption is expressed by Eq. 3:

$$\log q_e = \log K_F + 1/n \log C_e, \tag{3}$$

In this equation,  $K_F$  and  $1/n$  are Freundlich constant and favorability, respectively. These values were calculated by depiction of  $\log q_e$  versus  $\log C_e$  for MG and are presented in Table 1. The values of  $1/n$  are generally between 0 and 1 [41]. Based on the obtained results, the  $R^2$  values of Langmuir and Freundlich equations are 0.98 and 0.97, respectively, which show that the adsorption of MG on the rGO–PANI nanocomposite is obeyed by both adsorption isotherms.

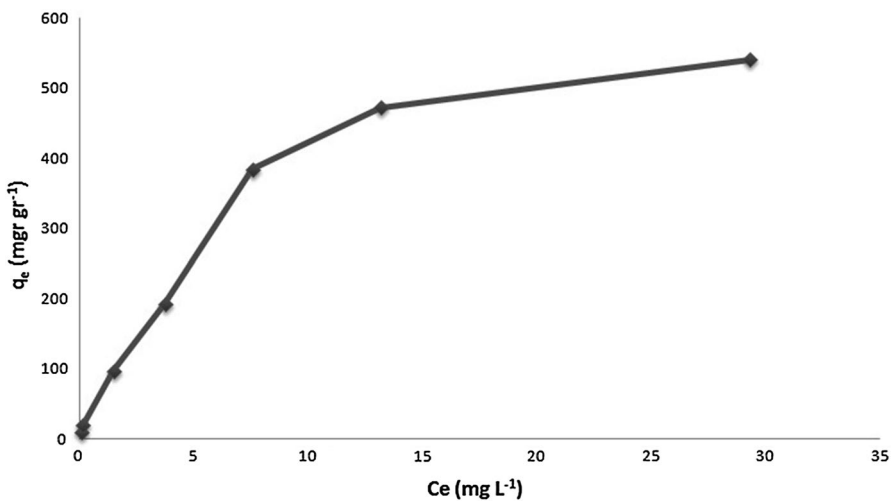


**Fig. 7** Plot of  $q_e$  versus  $C_e$ . (pH: 6, contact time: 20 min)

## Kinetic models for the adsorption of MG onto the rGO–PANI nanocomposite

### Pseudo-first-order equation

Equation 4 shows the pseudo-first-order kinetic model [42]:

$$\frac{dq_t}{dt} = k_1(q_e - q_t) \quad (4)$$

$$\text{Log}\left(\frac{q_e}{q_e - q_t}\right) = \frac{k_1}{2.303} \quad (5)$$

$$\text{Log}(q_e - q_t) = \log q_e - \frac{k_1}{2.303}t \quad (6)$$

Equations 5 and 6 are the linear forms of Eq. 4, where  $k_1$  is the rate constant in  $\text{min}^{-1}$ . By plotting of  $\log(q_e - q_t)$  versus  $t$  for MG (Fig. 8), the values of  $k_1$  and  $q_e$  could be determined from the slope and intercept of the plot, respectively. The results of  $R^2$ ,  $k_1$  and  $q_e$  for MG are shown in Table 2. As the results for different concentrations of MG show (10, 50, 100 and 200  $\text{mg L}^{-1}$  MG prepared by dilution of 0.5, 2.5, 5 and 10 mL of 1000  $\text{mg L}^{-1}$  MG to 50 mL with deionized water, respectively), the obtained  $R^2$  values ( $R^2 \geq 0.97$ ) indicate that the adsorption of MG is followed by pseudo-first-order kinetic model. Also, in pseudo-first-order kinetic system, the calculated  $q_e$  (cal) values are very close to the experimental  $q_e$  (Table 2), which clearly shows that the kinetic model for the adsorption of MG is governed by the pseudo-first-order kinetic model.

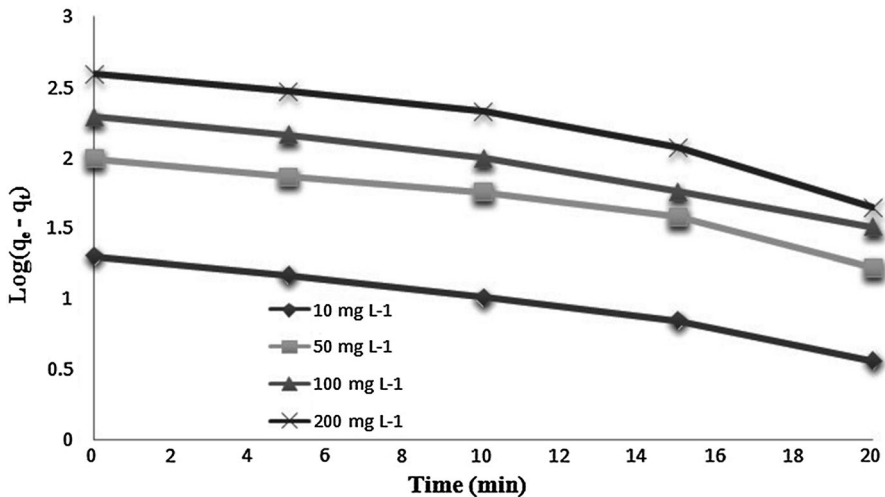


**Fig. 8** Pseudo-first-order kinetics for MG adsorption onto the rGO–PANI nanocomposite. Conditions: pH 6 and room temperature ( $25 \pm 2$  °C)

**Table 2** First-order adsorption rate constants and calculated and experimental  $q_e$  values for different initial MG concentrations

Dye	Concentration (mg L <sup>-1</sup> )	First-order kinetic model			
		$q_e$ (exp)	$q_e$ (cal)	$k_1$	$R^2$
Malachite green	10	19.7	21.4	0.083	0.975
	50	96.9	101.9	0.071	0.988
	100	192.5	214.3	0.091	0.981
	200	384.8	438.6	0.096	0.972

**Pseudo-second-order equation**

Another adsorption kinetic model is the pseudo-second-order kinetic model which is expressed by Eq. 7 [41]:

$$\frac{dq_t}{dt} = k_2(q_e - q_t)^2 \tag{7}$$

Its linear form is expressed by Eq. 8:

$$\frac{t}{q_t} = \frac{1}{k_2 q_e^2} + \frac{1}{q_e} t, \tag{8}$$

where  $k_2$  is the rate constant in  $g\ mg^{-1}\ min^{-1}$  and  $k_2 q_e^2$  is considered as  $h$  ( $h = k_2 q_e^2$ ), where  $h$  is the initial sorption rate in  $mg\ g^{-1}\ min^{-1}$ . The plot of  $t/q_t$  versus  $t$  is shown in Fig. 9, and the values of  $q_e$  and  $h$  could be obtained from the slope and intercept of the plot, respectively. Therefore, by determining  $q_e$ , the rate constant  $k_2$  could be determined from the intercept. The values of  $k_2$ ,  $h$  and  $R^2$  are demonstrated in

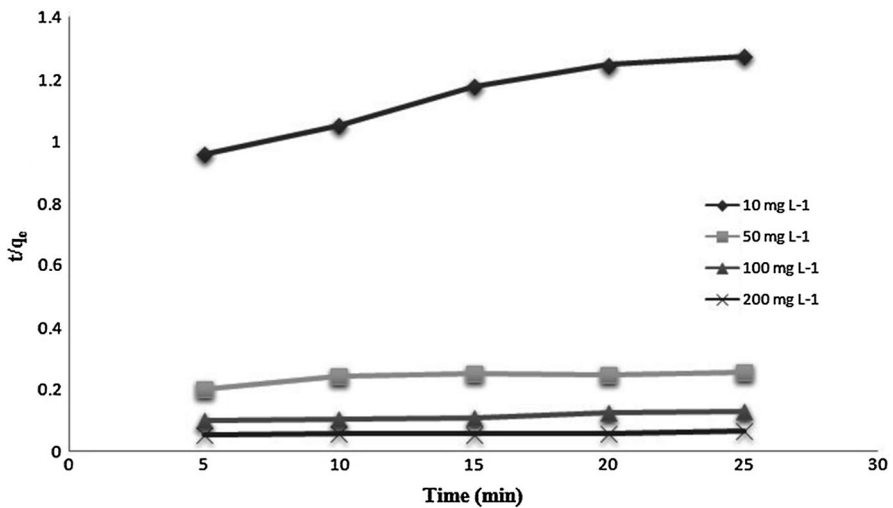


**Fig. 9** Pseudo-second-order kinetics for MG adsorption onto the rGO–PANI nanocomposite. Conditions: pH 6 and room temperature ( $25 \pm 2$  °C)

**Table 3** Second-order adsorption rate constants and calculated and experimental  $q_e$  values for different initial MG concentrations

Dye	Concentration (mg L <sup>-1</sup> )	Second-order kinetic model				
		$q_e$ (exp)	$q_e$ (cal)	$k_2$ ( $\times 0.001$ )	$h$	$R^2$
Malachite green	10	19.7	60.9	0.3	1.12	0.952
	50	96.9	325.6	0.0497	5.17	0.824
	100	192.5	652.7	0.0245	10.9	0.955
	200	384.8	1428.6	0.01038	21.2	0.805

**Table 4** Thermodynamic parameters for the adsorption of MG on rGO–PANI nanocomposite

$C_o$ (mg L <sup>-1</sup> )	$\Delta H^\circ$ (kJ mol <sup>-1</sup> )	$\Delta S^\circ$ (J mol <sup>-1</sup> K <sup>-1</sup> )	$\Delta G^\circ$ , 298.15 K (kJ mol <sup>-1</sup> )	$\Delta G^\circ$ (308.15) (kJmol <sup>-1</sup> )	$\Delta G^\circ$ (318.15) (kJ mol <sup>-1</sup> )
50	7.854	52.153	-7.695	-8.217	-8.738
100	8.089	51.895	-7.383	-7.902	-8.421

Table 3. Based on the results, the  $R^2$  values for MG are in the range of 0.80–0.95. Also, as it can be seen, the calculated  $q_e$  (cal) values for MG are far from the experimental  $q_e$  values (see Table 3). Therefore, the distance of experimental and theoretical ( $q_e$ ) values indicates that the pseudo-second-order kinetic model is not applicable for the prediction of adsorption data.

### Adsorption thermodynamics

In order to study the effect of temperature on the adsorption of MG, the thermodynamic parameters including standard Gibbs free energy change ( $\Delta G^\circ$ ), standard enthalpy changes ( $\Delta H^\circ$ ) and standard entropy changes ( $\Delta S^\circ$ ) are calculated from Eqs. 9–11 [5]:

$$\ln K_d = \frac{\Delta S^\circ}{R} - \frac{\Delta H^\circ}{RT}, \quad (9)$$

$$K_d = \frac{C_o - C_e}{C_e} \times \frac{V}{m}, \quad (10)$$

$$\Delta G = \Delta H - T\Delta S, \quad (11)$$

where  $K_d$ ,  $C_o$ ,  $C_e$ ,  $V$ ,  $m$ ,  $R$  and  $T$  are the distribution coefficient, initial and equilibrium concentrations of MG, volume of sample solution in Lit, amounts of adsorbent in g, universal gas constant (8.314 J mol<sup>-1</sup> K<sup>-1</sup>) and temperature in K, respectively. By depiction of  $\ln K_d$  versus  $1/T$ , the values of  $\Delta H^\circ$  and  $\Delta S^\circ$  could be determined from the slope and intercept of the plot, respectively (Table 4). As it could be seen, the negative  $\Delta G^\circ$  shows that the adsorption of MG onto the

**Table 5** Comparison of the adsorption capacities ( $Q_{\max}$ ) of MG onto various adsorbents

Adsorbent	pH	$Q_{\max}$ (mg g <sup>-1</sup> )	References
Fe <sub>3</sub> O <sub>4</sub> -β-CD-GO <sup>1</sup>	7	740.7	[5]
Activated carbon–lignite	7	200.0	[43]
Bentonite	5	178.6	[44]
Rice straw-derived char	5	148.7	[45]
Activated carbon/CoFe <sub>2</sub> O <sub>4</sub> composites	5	89.29	[8]
rGO–PANI nanocomposite	6	666.7	Present work

<sup>1</sup>Fe<sub>3</sub>O<sub>4</sub>-β-cyclodextrin-graphene oxide

rGO–PANI nanocomposite is spontaneous and the increase of the  $\Delta G^\circ$  values by increase of temperature shows that the adsorption process is desirable at higher temperatures. Also, the positive values of  $\Delta H^\circ$  show that the adsorption of MG onto the rGO–PANI nanocomposite is endothermic process.

### Comparison to other adsorbents

The efficiency of the proposed rGO–PANI nanocomposite for the removal of MG is shown in Table 5. The main advantages of rGO–PANI nanocomposite are novelty and high adsorption capacity for the removal of MG ( $Q_m = 666.7$  mg g<sup>-1</sup>) at only 20-min contact time which make it a powerful adsorbent for the removal of MG from water samples.

### Conclusion

In this research, rGO–PANI nanocomposite was used as an efficient and novel adsorbent for the removal of MG from water samples. GO was synthesized by Hummers' method, and after reduction and ultrasonication to rGO by NaBH<sub>4</sub>, its surface was modified by PANI to synthesize rGO–PANI nanocomposite. The synthesized rGO–PANI nanocomposite was then used as an adsorbent for the removal of MG from water samples. By optimizing critical parameters affecting the removal efficiency such as pH and contact time, kinetic models and adsorption isotherms were investigated and interpreted. The comparison of the efficiency of rGO–PANI nanocomposite by other adsorbents shows that it is a very efficient, highly rapid and novel adsorbent for the removal of MG from water samples. The investigation of two adsorption isotherms including Langmuir and Freundlich isotherms show that the adsorption of MG is obeyed by both Langmuir and Freundlich isotherms. Also, two kinetic models including the pseudo-first- and second-order equations were investigated and the results show that the adsorption of MG is governed by the pseudo-first-order kinetic equation. Finally, the results of thermodynamic study show that the adsorption of MG onto the rGO–PANI nanocomposite is endothermic and the negative values of  $\Delta G^\circ$  show that the adsorption of MG is spontaneous process.

**Acknowledgement** The authors thank the University of Neyshabur for financial support of this project. Also, we appreciated Mrs Melorin Eftekhari and Mahsa Keramati Yazadi.

## References

1. Reife A, Reife A, Freeman HS (1996) Environmental chemistry of dyes and pigments. Wiley, New York
2. Pereira L, Alves M (2012) Dyes—environmental impact and remediation. Springer, New York
3. Stolz A (2001) Basic and applied aspects in the microbial degradation of azo dyes. *Appl Microbiol Biotechnol* 56:69–80
4. Srivastava S, Sinha R, Roy D (2004) Toxicological effects of malachite green. *Aquat Toxicol* 66(3):319–329
5. Wang D, Liu L, Jiang X, Yu J, Chen X (2015) Adsorption and removal of malachite green from aqueous solution using magnetic  $\beta$ -cyclodextrin-graphene oxide nanocomposites as adsorbents. *Colloids Surf A, Physicochem Engin Aspect* 466:166–173
6. Sun H, Cao L, Lu L (2011) Magnetite/reduced graphene oxide nanocomposites: one step solvothermal synthesis and use as a novel platform for removal of dye pollutants. *Nano Res* 4(6):550–562
7. Mall ID, Srivastava VC, Kumar Agarwal N, Mani Mishra I (2005) Adsorptive removal of malachite green dye from aqueous solution by bagasse fly ash and activated carbon-kinetic study and equilibrium isotherm analyses. *Colloids Surf A: Physicochem Eng Asp* 264:17–28
8. Ai L, Huang H, Chen Z, Wei X, Jiang J (2010) Activated carbon/CoFe<sub>2</sub>O<sub>4</sub> composites: facile synthesis, magnetic performance and their potential application for the removal of malachite green from water. *Chem Engin J* 156:243–249
9. Garg VK, Kumar R, Gupta R (2004) Removal of malachite green dye from aqueous solution by adsorption using agro-industry waste: a case study of *Prosopis cineraria*. *Dyes Pigm* 62:1–10
10. Sartape AS, Mandhare AM, Jadhav VV, Raut PD, Anuse MA, Kolekar SS (2017) Removal of malachite green dye from aqueous solution with adsorption technique using *Limonia acidissima* (wood apple) shell as low cost adsorbent. *Arab J Chem* 10:S3229–S3238
11. Saygılı H, Güzel F (2015) Performance of new mesoporous carbon sorbent prepared from grape industrial processing wastes for malachite green and congo red removal. *Chem Engin Res Design* 100:27–38
12. Sadegh H, Shahyari-ghoshekandi R, Agarwal S, Tyagi I, Asif M, Kumar Gupta V (2015) Microwave-assisted removal of malachite green by carboxylate functionalized multi-walled carbon nanotubes: kinetics and equilibrium study. *J Mol Liq* 206:151–158
13. Han R, Wang Y, Sun Q, Wang L, Song J, He X, Dou C (2010) Malachite green adsorption onto natural zeolite and reuse by microwave irradiation. *J Hazard Mater* 175:1056–1061
14. Wu X, Wang Y, Liu J, Ma J, Han R (2010) Study of malachite green adsorption onto natural zeolite in a fixed-bed column. *Desalin Water Treat* 20:228–233
15. Khairud Dahri M, Rahimi Kooh MR, Kooh LBL (2014) Water remediation using low cost adsorbent walnut shell for removal of malachite green: equilibrium, kinetics, thermodynamic and regeneration studies. *J Environ Chem Engin* 2:1434–1444
16. Banerjee S, Sharma GC, Gautam RK, Chattopadhyaya MC, Upadhyay SN, Chandra Sharma Y (2016) Removal of Malachite Green, a hazardous dye from aqueous solutions using *Avena sativa* (oat) hull as a potential adsorbent. *J Mol Liq* 213:162–172
17. Jeyagowri B, Yamuna RT (2016) Potential efficacy of a mesoporous biosorbent *Simarouba glauca* seed shell powder for the removal of malachite green from aqueous solutions. *Desalin Water Treat* 57:11326–11336
18. Chen D, Feng H, Li J (2012) Graphene Oxide: preparation, Functionalization, and Electrochemical Applications. *Chem Rev* 112(11):6027–6053
19. Dahaghin Z, Zavvar Mousavi H, Sajjadi SM (2017) Synthesis and application of magnetic graphene oxide modified with 8-Hydroxyquinoline for extraction and preconcentration of trace heavy metal ions. *ChemistrySelect* 2(3):1282–1289
20. Eftekhari M, Gheibi M, Akrami M, Iranzad F (2018) Solid-phase extraction of ultra-trace levels of lead using tannic acid-coated graphene oxide as an efficient adsorbent followed by electrothermal atomic absorption spectrometry; response surface methodology-central composite design. *New J Chem* 42:1159–1168
21. Sun Z, James DK, Tour JM (2011) Graphene Chemistry: synthesis and Manipulation. *J Phys Chem Lett* 2:2425–2432
22. Pei S, Cheng HM (2012) The reduction of graphene oxide. *Carbon* 50:3210–3228

23. Yamani K, Berenguer R, Benyoucef A, Morallón E (2018) Preparation of polypyrrole (PPy)-derived polymer/ZrO<sub>2</sub> nanocomposites. In press, *J Therm Anal Calorim*
24. Iranzad F, Gheibi M, Eftekhari M (2018) Synthesis and application of polythiophene-coated Fe<sub>3</sub>O<sub>4</sub> nanoparticles for preconcentration of ultra-trace levels of cadmium in different real samples followed by electrothermal atomic absorption spectrometry. *Inter J Environ Anal Chem* 98(1):16–30
25. Zhan C, Yu G, Lu Y, Wang L, Wujcik E, Wei S (2017) Conductive polymer nanocomposites: a critical review of modern advanced devices. *J Mater Chem C* 5:1569–1585
26. Benyakhrou S, Belmokhtar A, Zehhaf A, Benyoucef A (2017) Development of novel hybrid materials based on poly(2-aminophenyl disulfide)/silica gel: preparation, characterization and electrochemical studies. *J Mol Struct* 1150:580–585
27. Sonkawade RG, Bagal IV, Chodankar NR, Waikar MR, Shinde PS, Shaikh AA (2018) Gamma irradiation: an efficient way to enhance current carrying properties of Ag/Ppy composite. *J Mater Sci: Mater Elec* 29:11151–11158
28. Stejskal J, Gilbert RG (2002) Polyaniline. Preparation of a conducting polymer. *Pure Appl Chem* 74(5): 857–867
29. Al-Kinani A, Eftekhari M, Gheibi M, Chamsaz M (2018) Polyaniline-coated cerium oxide nanoparticles as an efficient adsorbent for preconcentration of ultra-trace levels of cadmium (II) followed by electrothermal atomic absorption spectrometry. *Spectrosc Lett*, in press
30. Chiang JC, MacDiarmid AG (1986) Polyaniline: protonic acid doping of the emeraldine form to the metallic regime. *Synth Metals* 13(1–3):193–205
31. Huang WS, Humphrey BD, MacDiarmid AG (1986) Polyaniline, a novel conducting polymer. Morphology and chemistry of its oxidation and reduction in aqueous electrolytes. *J Chem Soc, Faraday Trans* 82:2385–2400
32. Daikh S, Zeggai FZ, Bellil A, Benyoucef A (2018) Chemical polymerization, characterization and electrochemical studies of PANI/ZnO doped with hydrochloric acid and/or zinc chloride: differences between the synthesized nanocomposites. *J Phys Chem Solids* 121:78–84
33. Pandiselvi K, Thambidurai S (2013) Synthesis of porous chitosan–polyaniline/ZnO hybrid composite and application for removal of reactive orange 16 dye. *Colloids Surf A* 108:229–238
34. Eisazadeh A, Eisazadeh H, AnuarKassim K (2013) Removal of Pb(II) using polyaniline composites and iron oxide coated natural sand and clay from aqueous solution. *Synth Met* 171:56–61
35. Benykhlef S, Bekhoukh A, Berenguer R, Benyoucef A, Morallón E (2016) PANI-derived polymer/Al<sub>2</sub>O<sub>3</sub> nanocomposites: synthesis, characterization, and electrochemical studies. *Colloid Polym Sci* 294:1877–1885
36. Wang Y, Zhang W, Wu X, Luo C, Wang Q, Li J, Hu L (2017) Conducting polymer coated metal-organic framework nanoparticles: facile synthesis and enhanced electromagnetic absorption properties. *Synth Met* 228:18–24
37. Shin HJ, Kim KK, Benayad A, Yoon SM, Park HK, Jung IS, Jin MH, Jeong HK, Kim JM, Choi JY, Lee YH (2009) Efficient reduction of graphite oxide by sodium borohydride and its effect on electrical conductance. *Adv Funct Mater* 19(12):1987–1992
38. Karandish S, Chamsaz M, Arbab Zavar MH, Gheibi M (2018) Reduced graphene oxide-polyaniline nanocomposite as an efficient adsorbent for solid phase extraction of Co<sup>2+</sup> followed by electrothermal atomic absorption spectrometry. *Inter J Environ Anal Chem* 98(12):1135–1148
39. Du XS, Zhou CF, Mai YW (2008) Facile synthesis of hierarchical polyaniline nanostructures with dendritic nanofibers as scaffolds. *J Phy Chem C* 112(50):19836–19840
40. Ibrahim KA (2017) Synthesis and characterization of polyaniline and poly(aniline-co-o-nitroaniline) using vibrational spectroscopy. *Arab J Chem* 10:S2668–S2674
41. Alpat SK, Ozbayrak O, Alpat S, Akcay H (2008) The adsorption kinetics and removal of cationic dye, Toluidine Blue O, from aqueous solution with Turkish zeolite. *J Hazard Mater* 151:213–220
42. Santhi T, Manonmani S, Smitha T (2010) Removal of malachite green from aqueous solution by activated carbon prepared from the epicarp of *Ricinus communis* by adsorption. *J Hazard Mater* 179:178–186
43. Onal Y, Akmil-Basar C, Sarici-Ozdemir C (2007) Investigation kinetics mechanisms of adsorption malachite green onto activated carbon. *J Hazard Mater* 146:194–203
44. Bulut E, Özacar M, Şengil İA (2008) Adsorption of malachite green onto bentonite: equilibrium and kinetic studies and process design. *Microporous Mesoporous Mater* 115:234–246
45. Hamed BH, El-Khaiary MI (2008) Kinetics and equilibrium studies of malachite green adsorption on rice straw-derived char. *J Hazard Mater* 153:701–708